*Int. J. Heat Mass Transfer.* Vol. 33, No. 7, pp. 1429–1440, 1990
Printed in Great Britain



# Near-wall modeling of turbulent heat fluxes

Y. G. LAI and R. M. C. SO
Mechanical and Aerospace Engineering, Arizona State University, Tempe, AZ 85287, U.S.A.

(*Received* 15 *April* 1989 *and in final form* 21 *September* 1989)

**Abstract**—The near-wall asymptotic behavior of the turbulent heat fluxes is analyzed and the result is used to formulate a second-moment turbulence closure for heat flux transport near a wall. The analysis shows that the pressure diffusion and viscous dissipation terms are of primary importance in the near-wall region and have to be properly modeled in the transport equations. New models satisfying the near-wall balance between viscous diffusion, viscous dissipation and pressure diffusion, and also having the characteristics of approaching their respective conventional high-Reynolds-number models far away from the wall are proposed. Fully-developed pipe flows with constant wall heat flux are chosen to validate the proposed models. The calculations show that the new models are capable of capturing the near-wall behavior very well. However, they also point to the rather immature status of the present high-Reynolds-number heat flux models. The modeling of the pressure-scrambling term is shown to have significant effects on the calculated heat flux and it is believed that this term is influenced by more than one turbulent time scale. Finally, the analysis also verifies the notion that the turbulent Prandtl number is not constant near a wall. If the turbulent Prandtl number is assumed constant, the results obtained are at variance with measurements.

## INTRODUCTION

WITH THE advent of high-speed computers, it is widely accepted that the isotropic diffusivity and wall function approach have to be abandoned for the calculation of complex turbulent flows [1–5]. This is especially the case for heat and mass transfer problems, even in simple pipe flows [1]. For non-buoyant flows, measurements (e.g. refs. [6, 7]) have shown that turbulent heat flux in the flow direction is two or three times larger than that normal to the wall, even though the streamwise temperature gradient is much smaller than its normal counterpart. For buoyant flows, the eddy diffusivity assumption is even less appropriate. Experimental measurements [8, 9] in a vertical heated pipe flow showed a substantial change in the turbulence structure, thus implying a reversal of the direction of the axial turbulent heat flux (i.e. the axial heat flux was measured upward instead of downward as implied by the eddy diffusivity concept). It is because of the above-mentioned reasons that many recent contributions to turbulence modeling are devoted to developing low-Reynolds-number turbulence closures [2, 10–12]. Although much progress has been achieved in recent years in the modeling of the Reynolds-stress transport equations [2], the modeling of the scalar field, on the other hand, is still rather primitive. The reason is that turbulent stresses are a very important input to the heat flux equations. Therefore, model development of the latter depends largely on the availability and correctness of the Reynolds-stress model. Furthermore, heat flux transport is influenced by more than one time scale [13]. Consequently, it is more difficult to achieve closure of the heat flux transport equations than the Reynolds-stress equations. Besides, a shortage of reliable and relatively accurate near-wall heat flux measurements also contributes to the slow development of a near-wall turbulence model for the heat fluxes. Comprehensive reviews of the modeling of turbulent heat transfer can be found in refs. [1, 14].

Due to the difficulties mentioned above, the most common approach to turbulent heat transfer studies is to model the normal heat flux using the classical Boussinesq approximation. The unknown eddy diffusivity for heat is calculated by prescribing a turbulent Prandtl number. Realizing the limitation of the calculation methods based on prescribed $Pr_t$, researchers try to improve the modeling by turning to two-equation [15] and algebraic flux models [16] for heat transport. Despite some successes, it is still believed that the most reliable prediction methods are those based on a second-moment closure. The reason is that the turbulent interactions which generate the Reynolds stresses and heat fluxes can be treated with less empiricism. Moreover, for those processes which cannot be so handled, a more rational and systematic set of approximations can be derived.

A first attempt to compute the turbulent heat transfer process using high-Reynolds-number second-moment closures was made by meteorological fluid dynamicists [17–19]. On the other hand, applications of similar second-moment turbulence closures to engineering heat transfer problems have been attempted by Baughn *et al.* [20] and Launder and Samaraweera [21], among others. Recently, the model was extended by Yoo and So [22] to calculate isothermal, variable-density flows in a sudden-expansion pipe. In their approach, the flow and turbulence field were resolved by a low-Reynolds-number second-

## NOMENCLATURE

$B_\theta$ intercept of the temperature log law
$c_p$ specific heat at constant pressure
$D$ pipe diameter
$k$ turbulent kinetic energy
$n_i$ unit normal to (and with origin at) the wall
$P, p$ mean and fluctuating static pressure
$Pr, Pr_t$ molecular and turbulent Prandtl number
$q_w$ wall heat flux
$r$ radial coordinate measured from pipe centerline
$R$ radius of the pipe
$Re$ Reynolds number, $u_\tau R/\nu$
$Re_m, Re_0$ Reynolds numbers, $U_m D/\nu$, $U_0 D/\nu$, respectively
$Re_t$ turbulent Reynolds number, $k^2/\nu\varepsilon$
$U_i, u_i$ $i$th component of the mean and fluctuating velocity
$U, u$ mean and fluctuating streamwise velocities
$U_m$ bulk mean axial velocity in the pipe
$U_0$ mean axial velocity at pipe centerline
$u_\tau$ wall friction velocity, $(\tau_w/\rho)^{1/2}$
$\overline{u_i u_j}$ Reynolds stress tensor
$\overline{u_i\theta}$ turbulent heat flux vector
$V, v$ mean and fluctuating velocities normal to the wall
$x$ streamwise coordinate
$x_i$ $i$th component of the Cartesian coordinate ($x_1$ streamwise, $x_2$ normal to the wall)
$y$ coordinate normal to (and with origin at) the wall
$y^+$ distance normal to the wall in standard wall coordinate, $yu_\tau/\nu$.

Greek symbols

$\alpha$ molecular heat diffusivity
$\varepsilon$ dissipation rate of $k$
$\varepsilon_\theta$ dissipation rate of $\frac{1}{2}\overline{\theta^2}$
$\Theta, \theta$ mean and fluctuating value of temperature
$\Theta_w$ wall temperature
$\Theta_\tau$ wall friction temperature, $q_w/\rho c_p u_\tau$
$\Theta^+$ mean temperature in wall coordinates, $(\Theta_w-\Theta)/\Theta_\tau$
$\kappa_\theta$ slope of temperature log law
$\nu$ molecular kinematic viscosity
$\rho$ fluid density
$\tau_w$ wall shear stress.

moment closure. The scalar flux equation was closed by high-Reynolds-number models and the near-wall scalar fluxes were evaluated assuming a constant turbulent Schmidt number. This is one way to handle the scalar flux transport equations for the near-wall flow, even though the approach is known to be quite inappropriate for most turbulent heat and mass transfer problems of engineering interest [1, 5, 22]. The reason for this appears to be that, so far, no suitable near-wall second-moment closure for scalar flux transport has been developed. This is due, in part, to a lack of detailed near-wall scalar flux measurements and, partially, to the unavailability of an asymptotically correct near-wall Reynolds-stress model.

Recently, Lai and So [2] have developed a near-wall Reynolds stress turbulence model that can correctly predict the anisotropy of the turbulent normal stresses. The success of that model provides the impetus to extend the approach of ref. [2] to model turbulent heat transport near a wall. It is noted, however, that detailed and accurate experimental documentation of buoyancy-dominated wall turbulent flow is presently not available and the modeling of the dissipation rate of temperature variance is quite immature, even the high-Reynolds-number version of the modeled equation is not well developed. In view of this, the present study will concentrate on the modeling of near-wall heat flux transport in the absence of any buoyancy effect in the flow. Therefore, the proposed near-wall heat flux model is equally valid for any passive scalar transport. The approach taken is similar to that outlined in ref. [2] and is based on the limiting wall behavior of the heat flux transport equations. This way, the modeled equation is valid all the way to the wall and the assumptions of a temperature wall function and a constant turbulent Prandtl number are not required. The proposed model is validated against fully-developed pipe flow data with uniform heat flux prescribed at the wall [6, 7, 23, 24]. The validation of the model for more complex flows will be carried out in the second phase of this study after a careful examination of the high-Reynolds-number models for the heat flux transport equations has been completed.

## MODELING OF THE REYNOLDS-STRESS EQUATIONS

The Reynolds-stress transport equations for an incompressible, non-buoyant turbulent flow can be concisely written as

$$C_{ij} = D^v_{ij} + D^t_{ij} + P_{ij} + \Phi^*_{ij} - \varepsilon_{ij}. \quad (1)$$

Detailed expressions for the above tensor forms and their modeling can be found in ref. [2]. Here, for convenience, the final forms of the models are given

as

$$D^t_{ij} = \frac{\partial}{\partial x_k}\left\{c_s \frac{k}{\varepsilon}\left[\overline{u_i u_l}\frac{\partial \overline{u_j u_k}}{\partial x_l} + \overline{u_j u_l}\frac{\partial \overline{u_k u_i}}{\partial x_l} + \overline{u_k u_l}\frac{\partial \overline{u_i u_j}}{\partial x_l}\right]\right\} \quad (2)$$

$$\varepsilon_{ij} = \tfrac{2}{3}\varepsilon(1-f_{w,1})\delta_{ij} + f_{w,1}\frac{\varepsilon}{k}[\overline{u_i u_j} + \overline{u_i u_k}n_k n_j + \overline{u_j u_k}n_k n_i + n_i n_j \overline{u_k u_l}n_k n_l]/[1+3\overline{u_k u_l}n_l n_k/2k] \quad (3)$$

$$\Phi^*_{ij} = \Phi_{ij} + \Phi_{ij,w} f_{w,1} \quad (4)$$

$$\Phi_{ij} = -c_1\frac{\varepsilon}{k}(\overline{u_i u_j} - \tfrac{2}{3}\delta_{ij}k) - \frac{(c_2+8)}{11}\left(P_{ij} - \frac{\delta_{ij}}{3}P_{kk}\right) - \frac{(8c_2-2)}{11}\left(D_{ij} - \frac{\delta_{ij}}{3}P_{kk}\right) - \frac{(30c_2-2)}{55}k\left(\frac{\partial U_i}{\partial x_j} + \frac{\partial U_j}{\partial x_i}\right) \quad (5)$$

$$\Phi_{ij,w} = c_1\frac{\varepsilon}{k}(\overline{u_i u_j} - \tfrac{2}{3}\delta_{ij}k) - \frac{\varepsilon}{k}(\overline{u_i u_k}n_k n_j + \overline{u_j u_k}n_k n_i) + \alpha^*\left(P_{ij} - \frac{\delta_{ij}}{3}P_{kk}\right) \quad (6)$$

where

$$P_{ij} = -\left\{\overline{u_i u_k}\frac{\partial U_j}{\partial x_k} + \overline{u_j u_k}\frac{\partial U_i}{\partial x_k}\right\} \quad (7a)$$

$$D_{ij} = \left\{\overline{u_i u_k}\frac{\partial U_k}{\partial x_j} + \overline{u_j u_k}\frac{\partial U_k}{\partial x_i}\right\} \quad (7b)$$

and the model constants are taken to be the same as those given in ref. [2], i.e. $c_1 = 1.5$, $c_2 = 0.4$, $c_s = 0.11$, $\alpha^* = 0.45$ and $f_{w,1} = \exp\{-(Re_t/150)^2\}$. The convective and viscous diffusive transport terms in equation (1) are defined as $C_{ij} = D\overline{u_i u_j}/Dt$ and $D^v_{ij} = \partial[\nu\partial\overline{u_i u_j}/\partial x_k]/\partial x_k$, respectively.

A transport equation for the dissipation rate $\varepsilon$ is required to complete the closure of the hydrodynamic flow. This equation is also taken from ref. [2] and is listed as follows:

$$\frac{D\varepsilon}{Dt} = \frac{\partial}{\partial x_k}\left(\nu\frac{\partial \varepsilon}{\partial x_k}\right) + \frac{\partial}{\partial x_k}\left(c_\varepsilon\frac{k}{\varepsilon}\overline{u_k u_i}\frac{\partial \varepsilon}{\partial x_i}\right) + c_{\varepsilon 1}(1+\sigma f_{w,2})\frac{\varepsilon}{2k}P_{kk} - c_{\varepsilon 2}f_\varepsilon\frac{\varepsilon\tilde{\varepsilon}}{k} + \xi \quad (8)$$

with

$$\sigma = 1.0 - 0.6\exp\left[-\frac{Re_m}{10^4}\right]$$

$$\xi = f_{w,2}\left[\left(\frac{7}{9}c_{\varepsilon 2} - 2\right)\frac{\varepsilon\tilde{\varepsilon}}{k} - \frac{1}{2}\frac{\varepsilon^{*2}}{k}\right]$$

and

$$\tilde{\varepsilon} = \varepsilon - 2\nu\left(\frac{\partial\sqrt{k}}{\partial y}\right)^2, \quad \varepsilon^* = \varepsilon - \frac{2\nu k}{y^2}.$$

The model constants are specified by ref. [2] as $c_\varepsilon = 0.15$, $c_{\varepsilon 1} = 1.35$ and $c_{\varepsilon 2} = 1.8$, and the damping functions are defined as

$$f_\varepsilon = 1 - \tfrac{2}{9}\exp\left\{-\left(\frac{Re_t}{6}\right)^2\right\}, \quad f_{w,2} = \exp\left\{-\left(\frac{Re_t}{64}\right)^2\right\}.$$

This is a new approach for equation (1) for near-wall turbulent flows. It can be seen from the proposed new models for $\varepsilon_{ij}$ and $\Phi^*_{ij}$ that as the flow moves away from a wall, $f_{w,1}$ quickly vanishes and the above closure for equation (1) reduces to the high-Reynolds-number model of Launder *et al.* [25]. However, Lai and So [2] have shown that the proposed new models not only replicate the near-wall anisotropic turbulence behavior accurately, but also give correct predictions of the budgets of the Reynolds-stress near a wall compared to the direct simulation results of Kim *et al.* [26] and Mansour *et al.* [27]. Therefore, the above Reynolds-stress closure serves as an excellent basis for extension to near-wall turbulent heat flux modeling.

## ASYMPTOTIC BEHAVIOR OF THE HEAT FLUX EQUATIONS

With the Reynolds-stress transport equations closed as suggested above, attention can now be focused on the extension of the approach of Lai and So to model the turbulent heat flux transport equations near a wall. In order to correctly model the transport process in the viscous wall layer, the limiting behavior of the various terms in the heat flux equations has to be analysed along the lines of ref. [2]. The heat flux transport equations can be obtained by adding the momentum equation for $u_i$ multiplied by $\theta$ to the equation for $\theta$ multipled by $u_i$. The resultant equation may be arranged in Cartesian tensor form as

$$\frac{\partial}{\partial x_k}(U_k\overline{u_i\theta}) = -\frac{\partial}{\partial x_k}(\overline{u_i u_k\theta}) + \frac{\partial}{\partial x_k}\left[\nu\overline{\theta\frac{\partial u_i}{\partial x_k}} + \alpha\overline{u_i\frac{\partial\theta}{\partial x_k}}\right] - \overline{u_i u_k}\frac{\partial\Theta}{\partial x_k} - \overline{u_k\theta}\frac{\partial U_i}{\partial x_k} - \overline{\frac{\theta}{\rho}\frac{\partial p}{\partial x_i}} - (\alpha+\nu)\overline{\frac{\partial\theta}{\partial x_k}\frac{\partial u_i}{\partial x_k}} \quad (9)$$

or symbolically as

$$C_{i\theta} = D^t_{i\theta} + D^v_{i\theta} + P_{i\theta,1} + P_{i\theta,2} + \Phi^*_{i\theta} - \varepsilon_{i\theta}. \quad (10)$$

The meaning of the terms in equation (10) from left to right are convective transport, turbulent diffusive transport, viscous diffusive transport, production by mean temperature gradient, production by mean shear, pressure scrambling and molecular dissipation of the heat fluxes.

Near a wall, the fluctuating quantities can be expanded in terms of $y$ as

Table 1. Near-wall behavior of heat flux equations

| | $C_{i\theta}$ | $-D^{\nu}_{i\theta}$ | $-D^{\nu}_{i\theta}$ | $-P_{i\theta,1}-P_{i\theta,2}$ | $\varepsilon_{i\theta}$ | $\Phi^{*}_{i\theta}$ |
|---|---|---|---|---|---|---|
| $i=1$ | | | $-(\alpha+\nu)\overline{a_1 d_1}$ | | $(\alpha+\nu)\overline{a_1 d_1}$ | |
| $(x)$ | $O(y^3)$ | $O(y^3)$ | $+O(y)$ | $O(y^3)$ | $+O(y)$ | $O(y)$ |
| $i=2$ | | | $-(4\nu+2\alpha)\overline{b_2 d_1}y$ | | $2(\alpha+\nu)\overline{b_2 d_1}y$ | |
| $(y)$ | $O(y^4)$ | $O(y^4)$ | $+O(y^2)$ | $O(y^4)$ | $+O(y^2)$ | $-2\nu\overline{b_2 d_1}y$ |
| $i=3$ | | | $-(\alpha+\nu)\overline{a_3 d_1}$ | | $(\alpha+\nu)\overline{a_3 d_1}$ | |
| $(z)$ | $O(y^3)$ | $O(y^3)$ | $+O(y)$ | $O(y^3)$ | $+O(y)$ | $O(y)$ |

$$
\begin{aligned}
u &= a_1 y + b_1 y^2 + \cdots \\
v &= \quad b_2 y^2 + \cdots \\
w &= a_3 y + b_3 y^2 + \cdots \\
\theta &= d_1 y + d_2 y^2 + \cdots
\end{aligned} \tag{11}
$$

where $u_i = (u, v, w)$ and $x_i = (x, y, z)$ are substituted for convenience, $x$ is the flow direction and $z$ is normal to the $x$–$y$ plane. The coefficients $a_i$, $b_i$, etc. are random functions of time and $x$ and $z$, and the expansion for $v$ starts with $y^2$ because of the incompressibility condition. The above expansions can now be substituted into the various expressions defining the terms in equation (10) except $\Phi^{*}_{i\theta}$. Consequently, the asymptotic behavior of the various terms in equation (10) except $\Phi^{*}_{i\theta}$ can be determined and the balance of equation (10) can be taken to define the asymptotic behavior of $\Phi^{*}_{i\theta}$. The result, written out to the lowest order for each term in equation (10) is given in Table 1. With the guide of these near-wall values, a new low-Reynolds-number turbulent heat flux model can be constructed. Thus formulated, the new heat flux model is consistent with the near-wall Reynolds-stress model, and together they give an asymptotically correct near-wall turbulence model for heat and mass transfer studies.

## MODELING OF THE HEAT FLUX EQUATIONS

As can be seen from Table 1, the influence of turbulent diffusion is negligible near a wall. This has actually been confirmed in the present calculation of a fully-developed, heated pipe flow. Therefore, consistent with the near-wall Reynolds-stress model [2], the high-Reynolds-number assumption is invoked in the modeling of the turbulent diffusion term. Various high-Reynolds-number heat flux diffusion models are available in the literature, e.g. Owen [28], Launder [29] and Donaldson *et al.* [30], among others. A comprehensive review of these models is given in ref. [14]. Later, a more elaborate heat flux diffusion model was suggested by Lumley [31]. Since the choice of a diffusion model only has noticeable influence near the central portion of the pipe flow, it is not a critical issue for the near-wall flow. Therefore, the model suggested by Launder [29] is adopted, or

$$
-\overline{u_i u_k \theta} = c_s^{\theta} \frac{k}{\varepsilon} \left( \overline{u_i u_l} \frac{\partial \overline{u_k \theta}}{\partial x_l} + \overline{u_k u_l} \frac{\partial \overline{u_i \theta}}{\partial x_l} \right). \tag{12}
$$

This particular form is chosen because it gives the best overall agreement with data compared to other versions considered in ref. [21]. The recommended values of $c_s^{\theta}$ are 0.11 according to Launder and Samaraweera [21] and 0.20 according to refs. [14, 28, 29]. In the present study, 0.11 is chosen because it gives the best correlation with fully-developed, heated pipe flow measurements.

Contrary to the near-wall Reynolds-stress model, the molecular diffusion term is not of the correct form. Therefore, it also needs 'modeling'. $D^{\nu}_{i\theta}$ can be rearranged as

$$
D^{\nu}_{i\theta} = \frac{\partial}{\partial x_k} \left[ \nu \frac{\partial \overline{u_i \theta}}{\partial x_k} + (\alpha - \nu) \overline{u_i \frac{\partial \theta}{\partial x_k}} \right]. \tag{13}
$$

Based on the asymptotic behavior shown in Table 1, the right-hand side of (13) can be 'modeled' as

$$
D^{\nu}_{i\theta} = \nu \frac{\partial^2 \overline{u_i \theta}}{\partial x_k^2} + \frac{\alpha - \nu}{n_i + 2} \frac{\partial^2 \overline{u_i \theta}}{\partial x_k^2} \quad \text{(no summation for } i\text{)}. \tag{14}
$$

As for the dissipation term, it is usually assumed that turbulence is isotropic for high-Reynolds-number flows and consequently it is zero because there is no isotropic first-order tensor. However, for near-wall flows, where the Reynolds number is no longer large, the dissipation term becomes important. In fact, the limiting values listed in Table 1 show that viscous dissipation is of primary importance near a wall and provides all or part of the balance to molecular diffusion. Similar to the modeling of $\varepsilon_{ij}$, $\varepsilon_{i\theta}$ is modeled in such a way that it will go to zero far away from the wall and approach its asymptotic value near the wall. An expression satisfying the above constraints can be proposed as

$$
\varepsilon_{i\theta} = \tfrac{1}{2} f_{w,0} \left( 1 + \frac{1}{Pr} \right) \frac{\varepsilon}{k} [\overline{u_i \theta} + \overline{u_k \theta} n_k n_i] \tag{15}
$$

where $Pr$ is the molecular Prandtl number and $f_{w,\theta}$ a damping function taken to be $\exp[-(Re_t/80)^2]$.

The modeling of $\Phi_{i\theta}^*$ also follows the approach outlined in ref. [2], such that

$$\Phi_{i\theta}^* = \Phi_{i\theta} + f_{w,\theta}\Phi_{i\theta,w}^*. \tag{16}$$

In equation (16), $\Phi_{i\theta}$ represents the conventional high-Reynolds-number model of pressure-scrambling, while the complete model satisfies the near-wall behavior shown in Table 1 and the lowest order balance between molecular diffusion, dissipation and pressure diffusion near a wall. It should be noted that the $\Phi_{i\theta}$ models proposed so far are not as well formulated as the corresponding $\Phi_{ij}$ models because of the inherent difficulties encountered in heat flux modeling. Even then, three different contributions to the $\Phi_{i\theta}$ term can be identified. These contributions are due to turbulence fluctuations, mean strain and wall reflection of the fluctuation pressure. Symbolically, the model for $\Phi_{i\theta}$ can be written as

$$\Phi_{i\theta} = \Phi_{i\theta,1} + \Phi_{i\theta,2} + \Phi_{i\theta,w} \tag{17}$$

where $\Phi_{i\theta,1}$ represents the fluctuating contribution, $\Phi_{i\theta,2}$ the mean strain contribution and $\Phi_{i\theta,w}$ the wall reflection contribution. The most popular model for $\Phi_{i\theta,1}$ is that proposed by Monin [17] and adopted by nearly all subsequent researchers; namely

$$\Phi_{i\theta,1} = -c_{1\theta}\frac{\varepsilon}{k}\overline{u_i\theta} \tag{18}$$

where only one time scale ($k/\varepsilon$) is used in spite of the suggestion by Launder [14] that the time scale for $\Phi_{i\theta,1}$ should also include the effect of $\overline{\theta^2}/\varepsilon_\theta$. It is worth noting that Shih and Lumley [13] have recently pointed out that $c_{1\theta}$ cannot be a universal constant for different turbulent flows and proceeded to develop a functional relationship between $c_{1\theta}$ and the time scale ratio. In spite of this, the present study will adopt a constant value of $c_{1\theta} = 3.0$ as suggested in ref. [1]. The reason is that the simple model given by equation (18) has been validated against free shear flows as well as wall-bounded turbulent flows. On the other hand, the more elaborate model of ref. [13] has not been sufficiently validated for general applications. A second reason is that the present concern is with the near-wall asymptotic behavior rather than with the high-Reynolds-number model. Besides, it is believed that the present approach to construct a near-wall turbulent heat flux model can be easily extended when a more fundamental and suitable model for the pressure-scrambling term is available.

It seems that no such ambiguity exists for the modeling of the mean strain term, $\Phi_{i\theta,2}$. Among two models in common use, the destruction of production model [14] seems to give a more satisfactory approximation of highly sheared flows [21] compared to the quasi-isotropic model [29]. The destruction of production model can be written as

$$\Phi_{i\theta,2} = -c_{2\theta}P_{i\theta,2} = c_{2\theta}\overline{u_k\theta}\frac{\partial U_i}{\partial x_k} \tag{19}$$

with the model constant $c_{2\theta}$ given by 0.4 as suggested in ref. [1].

The importance of the wall reflection term was pointed out in ref. [21]. Therefore, its influence on near-wall turbulent heat flux modeling is also examined in the present study. As a first attempt, the model proposed in ref. [1] is adopted, or

$$\Phi_{i\theta,w} = -c_{1\theta,w}\frac{\varepsilon}{k}\overline{u_k\theta}n_k n_i\frac{k^{3/2}}{\varepsilon y} \tag{20}$$

where the coefficient $c_{1\theta,w}$ is taken to be 0.75. Analysis with and without the presence of this term in equation (17) will be carried out and their results compared with measurements. In summary, the selection of the various models for the pressure-scrambling term follows closely those suggested in ref. [1]. The model constants are not varied to fit the experimental data. Instead, the present objective is to formulate a model for $\Phi_{i\theta,w}^*$ so that the asymptotic behavior of $\Phi_{i\theta}^*$ near a wall is correctly reproduced.

It can easily be shown that the lowest term in the model for $\Phi_{i\theta,1}$ is finite along the stream direction. On the other hand, the lowest order term in the models for $\Phi_{i\theta,2}$ and $\Phi_{i\theta,w}$ is of order $y^n$ where $n \geq 3$. Therefore, near a wall, the model for $\Phi_{i\theta,w}^*$ has to provide terms to balance this behavior so that the final model for $\Phi_{i\theta}^*$ will come out to behave like that shown in Table 1. A careful analysis leads to the following model for $\Phi_{i\theta,w}^*$, or

$$\Phi_{i\theta,w}^* = c_{1\theta}\frac{\varepsilon}{k}\overline{u_i\theta} - \frac{\varepsilon}{k}\overline{u_k\theta}n_k n_i. \tag{21}$$

With the model for $\Phi_{i\theta}^*$ defined, a new near-wall turbulence closure for equation (9) is now available. The closure asymptotes correctly to the high-Reynolds-number closure far away from the wall. Thus formulated, the calculation can be carried out all the way to the wall without the need to invoke empirical wall functions and a constant Prandtl/Schmidt number. Finally, it should be pointed out that the high-Reynolds-number model for the pressure-scrambling term can be replaced by a more appropriate model when one becomes available and the model for $\Phi_{i\theta,w}^*$ can be formulated by following the procedure outlined above for the derivation of equation (21). Thus, model (21) may not be universal, but the methodology is indeed very general.

## GOVERNING EQUATIONS AND COMPUTATIONAL DETAILS

The near-wall heat flux model formulated above is used to study fully-developed, non-buoyant pipe flow subject to a constant wall heat flux condition. Comparisons are made with the available measurements of Johnk and Hanratty [23], Bremhorst and Bullock [6, 7] and Hishida *et al.* [24] for air flows with Reynolds number (based on pipe diameter and bulk mean velocity) ranging from 21 000 to 71 000. A cylindrical

coordinate system is chosen to describe the flow. The mean and fluctuating velocity and temperature are given by $(U, 0, 0)$, $(u, v, w)$, $\Theta$ and $\theta$, respectively. Since the governing equations for the hydrodynamic part of the flow are already provided in ref. [2], only the thermal energy and heat flux equations are given here. Written in terms of the models discussed above, these equations become

$$\alpha\frac{1}{r}\frac{\partial}{\partial r}\left(r\frac{\partial\Theta}{\partial r}\right)-\frac{1}{r}\frac{\mathrm{d}}{\mathrm{d}r}(r\overline{v\theta})=U\frac{\partial\Theta}{\partial x} \tag{22}$$

$$\begin{aligned}&\frac{1}{r}\frac{\mathrm{d}}{\mathrm{d}r}\left[r\left(\nu+\frac{\alpha-\nu}{3}+2c_s^{\theta}\frac{k}{\varepsilon}\overline{v^2}\right)\frac{\mathrm{d}\overline{v\theta}}{\mathrm{d}r}\right]\\&\quad-\frac{2}{r}c_s^{\theta}\frac{k}{\varepsilon}\overline{w^2}\frac{\overline{v\theta}}{r}-\left(\nu+\frac{\alpha-\nu}{3}\right)\frac{\overline{v\theta}}{r^2}-\overline{v^2}\frac{\partial\Theta}{\partial r}-\overline{uv}\frac{\partial\Theta}{\partial x}\\&\quad-(1-f_{w,\theta})c_{1\theta}\frac{\varepsilon}{k}\overline{v\theta}-c_{1\theta,w}\frac{\sqrt{k}}{R-r}\overline{v\theta}\\&\quad-f_{w,\theta}\frac{\varepsilon}{k}\overline{v\theta}-f_{w,\theta}\left(1+\frac{1}{Pr}\right)\frac{\varepsilon}{k}\overline{v\theta}=0\end{aligned} \tag{23}$$

$$\begin{aligned}&\frac{1}{r}\frac{\mathrm{d}}{\mathrm{d}r}\left[r\left(\nu+\frac{\alpha-\nu}{2}+c_s^{\theta}\frac{k}{\varepsilon}\overline{v^2}\right)\frac{\mathrm{d}\overline{u\theta}}{\mathrm{d}r}\right]\\&\quad+\frac{1}{r}\frac{\mathrm{d}}{\mathrm{d}r}\left[rc_s^{\theta}\frac{k}{\varepsilon}\overline{uv}\frac{\mathrm{d}\overline{v\theta}}{\mathrm{d}r}\right]-\overline{uv}\frac{\partial\Theta}{\partial r}-\overline{u^2}\frac{\partial\Theta}{\partial x}\\&\quad-\overline{v\theta}\frac{\mathrm{d}U}{\mathrm{d}r}-(1-f_{w,\theta})c_{1\theta}\frac{\varepsilon}{k}\overline{u\theta}+c_{2\theta}\overline{v\theta}\frac{\mathrm{d}U}{\mathrm{d}r}\\&\quad-\frac{f_{w,\theta}}{2}\left(1+\frac{1}{Pr}\right)\frac{\varepsilon}{k}\overline{u\theta}=0.\end{aligned} \tag{24}$$

Since the flow is axisymmetric, only the boundary conditions at the wall and the symmetry line are required to be specified. These are

$$\begin{aligned}&U=\overline{u^2}=\overline{v^2}=\overline{w^2}=\overline{uv}=0,\\&\varepsilon=2\nu\left(\frac{\partial\sqrt{k}}{\partial y}\right)^2\quad\text{at } r=R\\&\Theta=\Theta_w,\quad\overline{v\theta}=\overline{u\theta}=0\quad\text{at } r=R\\&\frac{\mathrm{d}\varepsilon}{\mathrm{d}r}=\frac{\mathrm{d}\overline{u^2}}{\mathrm{d}r}=\frac{\mathrm{d}\overline{v^2}}{\mathrm{d}r}=\frac{\mathrm{d}\overline{w^2}}{\mathrm{d}r}=0,\quad\overline{uv}=0\quad\text{at } r=0\\&\frac{\partial\Theta}{\partial r}=\frac{\mathrm{d}\overline{u\theta}}{\mathrm{d}r}=0,\quad\overline{v\theta}=0\quad\text{at } r=0.\end{aligned} \tag{25}$$

Note that an energy balance analysis over a control volume between $x$ and $x+\mathrm{d}x$ and the fully-developed condition gives

$$\frac{\mathrm{d}\Theta_w}{\mathrm{d}x}=\frac{\partial\Theta}{\partial x}=\frac{2q_w}{\rho c_p U_m R}. \tag{26}$$

Consequently, the final governing equations become a set of ordinary differential equations when the temperature difference, $(\Theta_w-\Theta)$, is used as the dependent variable. As such, the set of governing equations can be solved by the same numerical method described in ref. [32].

According to this numerical method [32], the set of governing equations with appropriate boundary conditions is solved numerically by the Newton iteration scheme. The solution is carried out with the dependent and independent variables normalized in the following manner: $U$ by $u_\tau$, $\overline{u_iu_j}$ by $u_\tau^2$, $\varepsilon$ by $u_\tau^3/R$, $(\Theta_w-\Theta)$ by $\Theta_\tau$, $\overline{u_i\theta}$ by $u_\tau\Theta_\tau$ and $y$ (or $R-r$) by $\nu/u_\tau$. Therefore, the integration from $r=0$ to $R$ is now carried out from $y^+=0$ to $Re$. Since $Re$ is related to $Re_0$ or $Re_m$ by $Re=(u_\tau/2U_0)Re_0$ or $Re=(u_\tau/2U_m)Re_m$, $Re$ becomes one of the two input parameters to the problem. The other input parameter is the molecular Prandtl number $Pr$. The eight second-order and one first-order ordinary differential equations are then written into 17 first-order equations by defining new variables for $\mathrm{d}(\overline{u_iu_j}/u_\tau^2)/\mathrm{d}y^+$, $\mathrm{d}(\varepsilon R/u_\tau^3)/\mathrm{d}y^+$, $\mathrm{d}(\overline{u_i\theta}/u_\tau\Theta_\tau)/\mathrm{d}y^+$ and $\mathrm{d}[(\Theta_w-\Theta)/\Theta_w]/\mathrm{d}y^+$. All the derivatives are approximated by centered-difference gradients and the resultant finite difference, non-linear algebraic equations are linearized using Newton's linearization scheme. The linearized algebraic equations together with the boundary conditions can be put into a block tri-diagonal matrix form and solved iteratively using any matrix inversion technique. Since the velocity and temperature fields are decoupled for non-buoyant flows, the velocity field can be solved first, followed by the temperature field. Iteration is carried out until the maximum relative change of all the variables at every grid point satisfies an accuracy criterion of $10^{-4}$ or less. A non-uniform grid is used to carry out the calculations. Five grid points are specified for $0\leqslant y^+\leqslant 5$ and 15 grid points are located in $5\leqslant y^+\leqslant 65$. The rest of the region $65\leqslant y^+\leqslant Re$ is then divided into 30–50 grid points depending on the problem considered. In general, this grid system is sufficient to give a convergent solution after 1500 iterations.

## RESULTS AND DISCUSSION

In order to validate the present near-wall turbulent heat flux model, several fully-developed pipe flow measurements with constant wall heat flux boundary conditions are chosen. These are the data of Bremhorst and Bullock [6, 7] with an $Re_0=69\,400$; Johnk and Hanratty [23] with three different Reynolds numbers given by $Re_m=24\,900$, 49 500 and 71 200; and finally Hishida *et al.* [24] with an $Re_m=40\,000$.

The calculations are carried out to assess the correctness and validity of the near-wall heat flux closure, the appropriateness of a turbulent Prandtl number formulation for normal heat flux and the effects of the various high-Reynolds-number pressure-scrambling models on the calculated results. In order to achieve these objectives, three different sets of calculations are performed. The first two sets are carried out using near-wall turbulent closures for both the Reynolds-stresses and heat fluxes. One major difference between

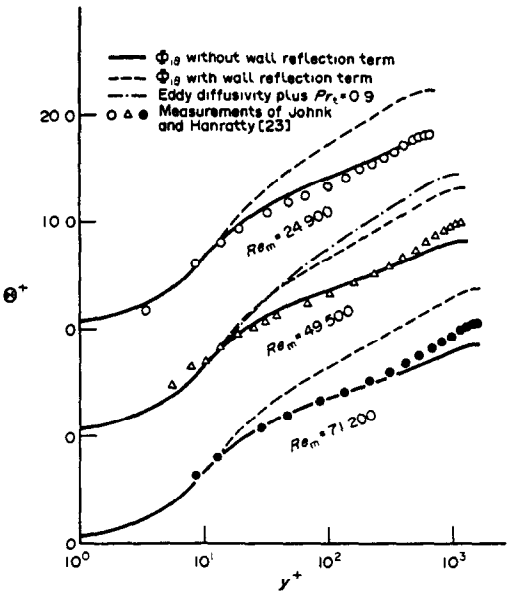


FIG. 1. Comparison of measured and calculated mean normalized temperatures in wall coordinates.

the first two sets of calculations is the handling of the wall reflection term in equation (17). In one set, the wall reflection term is included in the model, while the other set omits the contribution of this term. The third set relies on the near-wall Reynolds-stress closure to calculate $\overline{u_i u_j}$, while $\overline{v\theta}$ is obtained from

$$-\overline{v\theta} = \frac{\nu_t}{Pr_t}\frac{\partial \Theta}{\partial y} \tag{27}$$

with $\nu_t = c_\mu f_\mu k^2/\varepsilon$, $f_\mu = 1-\exp(-0.0115y^+)$ and $Pr_t = 0.9$ specified. A comparison of the three different sets of calculations with measurements will allow the relative strengths and weaknesses of the three different approaches of modeling turbulent heat transport to be assessed.

The most important comparison is with the normalized temperature profile plotted in wall coordinates. This comparison, therefore, is first made with the data of Johnk and Hanratty [23] for three different Reynolds numbers as shown in Fig. 1. In order to explore the influence of the wall reflection term, two calculations are presented for each Reynolds number; one with and one without $\Phi_{i\theta,w}$. The results show that the thermal viscous sublayer is not affected by the wall reflection term while the rest of the flow region is very much dependent on the model for $\Phi_{i\theta,w}$. It can be concluded that the wall reflection term (20) is unnecessary, at least when equations (18) and (19) are adopted for the pressure-scrambling model. More will be said about this wall reflection term when comparisons of other quantities with measurements are discussed.

It is clear that the predictions without the wall reflection term in equation (17) agree quite well with measurements, particularly for the thermal viscous sublayer, the buffer layer and the log law region. As a result, the slope and intercept of the temperature log law are very well reproduced by the calculations. The temperature log law is given by

$$\Theta^+ = \kappa_\theta^{-1} \ln y^+ + B_\theta. \tag{28}$$

From the results shown in Fig. 1, $(\kappa_\theta, B_\theta)$ are determined to be (0.47, 4.69), (0.51, 4.87) and (0.55, 5.37), respectively, for $Re_m = 24\,900$, 49 500 and 71 200. These values are in agreement with measurements and reaffirm the dependence of $\kappa_\theta$ and $B_\theta$ on Reynolds number. However, some discrepancy exists in the central part of the pipe. It is believed that the discrepancy comes about as a result of the incorrect high-Reynolds-number modeling of the pressure-scrambling and diffusion terms.

Besides the mean temperature field, the closure should also be assessed for its ability to predict the heat fluxes, $\overline{u\theta}$ and $\overline{v\theta}$. It is unfortunate that accurate experimental data for heat fluxes is not as well documented as Reynolds stresses. Therefore, the present comparison has to be carried out with the data of Bremhorst and Bullock [6, 7], which is not known for its accuracy, and with the data of Hishida *et al.* [24], which provides a very detailed measurement of the normal heat flux near a wall. The measurements of refs. [6, 7] are not exactly buoyant-free and the flow is affected by buoyancy as a result of the horizontal arrangement of the test rig and heat addition. In Figs. 2–4, the mean temperature, shear stress and normal

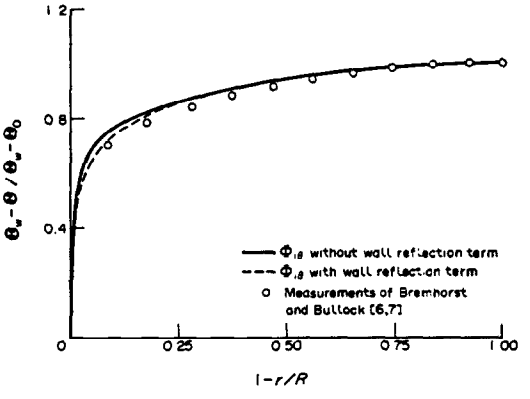


FIG. 2. Comparison of measured and calculated mean normalized temperatures.

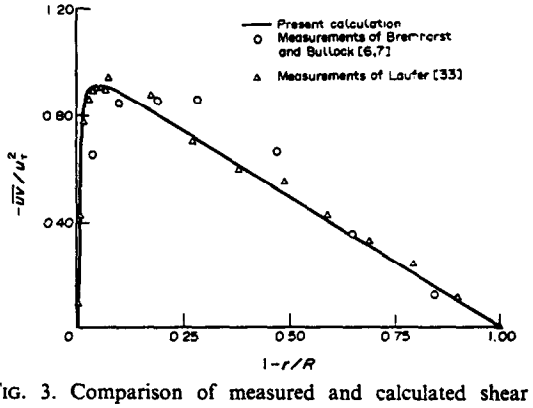


FIG. 3. Comparison of measured and calculated shear stresses.

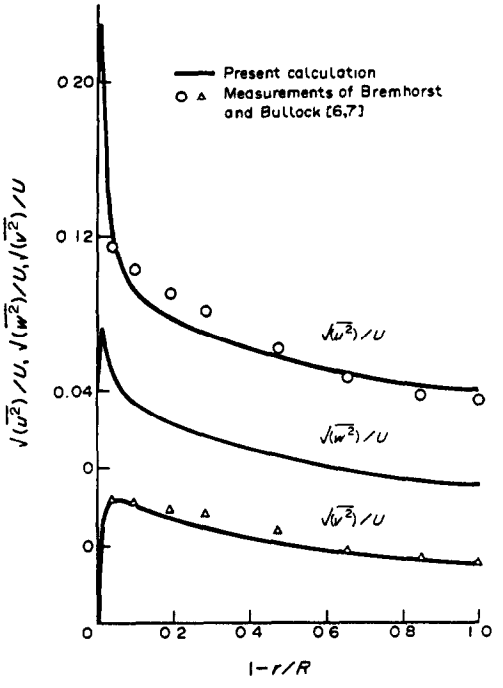


FIG. 4. Comparison of measured and calculated normal stresses.

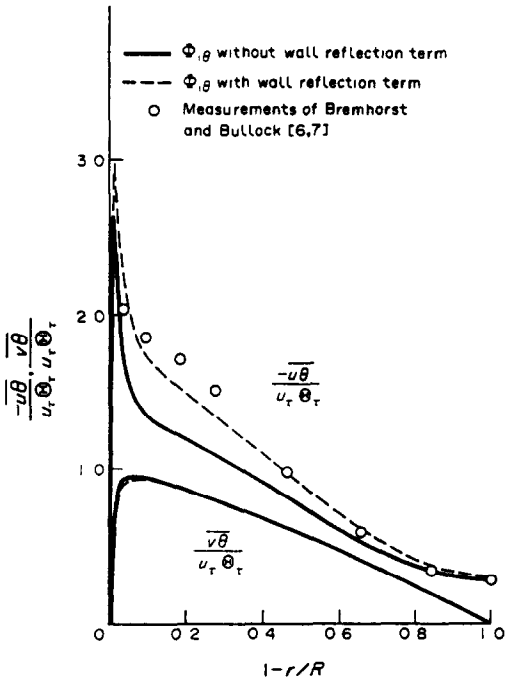


FIG. 5. Comparison of measured and calculated turbulent heat fluxes.

stresses are compared. It is noted that, in spite of the good agreement achieved in the prediction of the normal stresses (Fig. 4), the shear stress comparison shows a substantial and large discrepancy (Fig. 3). In view of this, the shear stress measurement of Laufer [33] at $Re_0 = 50\,000$ is also plotted in Fig. 3 for comparison. Lai and So [2] have shown that shear stress prediction is not much affected by the Reynolds number and excellent agreement with measurements is achieved using their near-wall Reynolds-stress closure. The discrepancy shown in Fig. 3 should therefore be interpreted as measurement distortion due to poor spatial resolution, as pointed out in refs. [6, 7]. Furthermore, Bremhorst and Bullock [6, 7] found that their measured shear stress does not agree with that calculated from the measured mean velocity profile, while the latter agrees well with the present calculation. Finally, it should be pointed out that a comparison of the linear plot of the normalized mean temperature shows that the prediction with wall reflection present is in better agreement with measurements (Fig. 2). This seems to contradict the results shown in Fig. 1. The reason is that the predicted $\Theta_\tau$ is incorrect. More will be said about this in the next paragraph.

The comparisons of the calculated and measured turbulent heat fluxes are shown in Fig. 5. Interestingly, these plots substantiate the result shown in Fig. 2; namely, that the pressure-scrambling model with the wall reflection term included correlates much better with measurements than the model with the wall reflection term absent. This may be part of the reason why this wall reflection term was introduced in the past. In fact, 'better' agreement in Fig. 2 is due to the normalization by $(\Theta_w - \Theta_0)$ and this ensures that $(\Theta_w - \Theta)/(\Theta_w - \Theta_0)$ varies from 0 to 1 in the flow region. As for the streamwise turbulent heat flux, the discrepancy between the model calculation with the wall reflection term absent and the measurement could be attributed to measurement errors generated by flow distortion due to buoyancy, and also partly to the simple one-time-scale model of pressure-scrambling. Shih and Lumley [13] argued that the pressure-scrambling process is influenced by more than one time scale and proceeded to propose modifications to the pressure-scrambling model. Similar arguments and proposals have also been made by Elghobashi and Launder [34]. However, most of these modifications are concerned only with homogeneous turbulent flows and are completely *ad hoc* [35]. Since these modifications have not been thoroughly tested, the present study will not attempt to further explore the effects of pressure-scrambling modeling. When new and more sophisticated models are available, the present approach can again be used to derive an asymptotically correct near-wall turbulent heat flux model.

Since near-wall measurements of the normal heat flux are recently available [24], this quantity is compared in Fig. 6. This comparison lends credence to the argument that the wall reflection term is not necessary in the model for $\Phi_{i\theta}^*$. In the absence of the wall reflection term, excellent agreement is obtained between the calculated and measured mean temperature profiles as well as the normal heat flux in the near-wall region

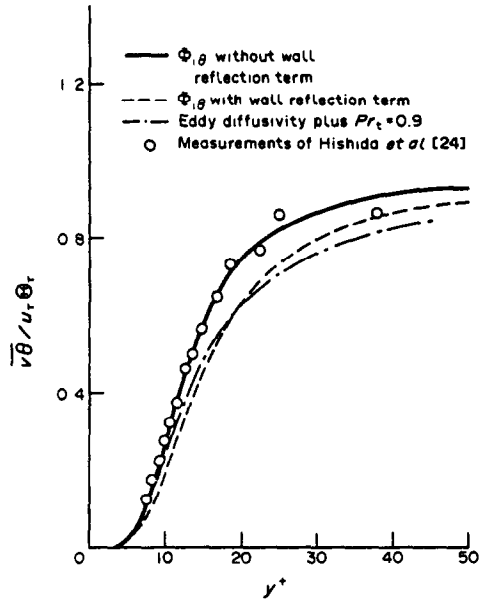


FIG. 6. Comparison of measured and calculated normal heat fluxes in the near-wall region.

(Figs. 1 and 6). Further evidence that the wall reflection term in $\Phi^*_{i\theta}$ is inappropriate can be obtained from the prediction of $-\overline{u\theta}/\overline{v\theta}$ (Fig. 7). In the central portion of the pipe, this ratio is approximately 1.33 for the calculation without the wall reflection term present, while it is about 1.7 and not quite constant for the case with the wall reflection term present. The analysis in ref. [14] for two-dimensional thin shear flow showed that the measurements of Champagne *et al.* [36] give

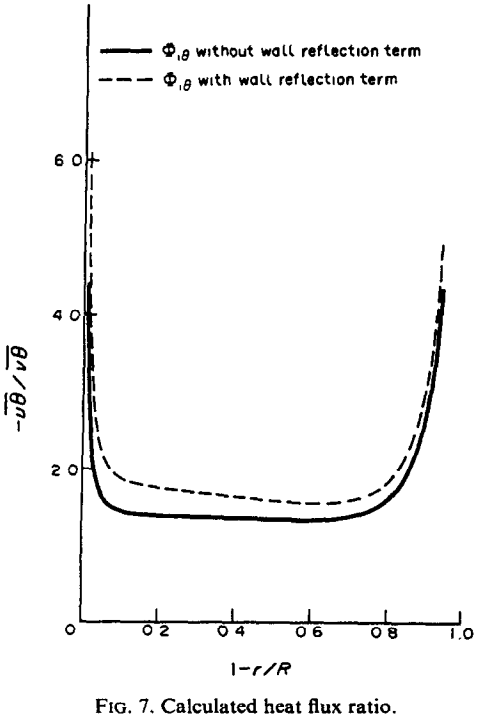


FIG. 7. Calculated heat flux ratio.

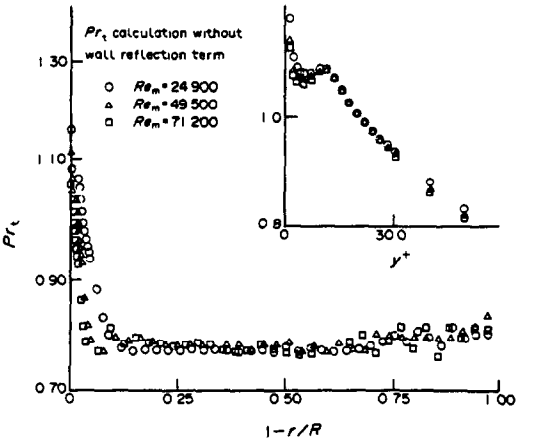


FIG. 8. Behavior of the calculated turbulent Prandtl number.

a value of 1.27. Therefore, the $-\overline{u\theta}/\overline{v\theta}$ data support the neglect of the wall reflection term in the modeling of $\Phi^*_{i\theta}$.

The calculated turbulent Prandtl numbers for three different Reynolds numbers are shown in Fig. 8. It is observed that $Pr_t$ is approximately constant for the most part of the pipe. However, it increases steeply and far exceeds unity as the wall is approached. This behavior is consistent with the flat-plate boundary-layer measurements of Johnson [37] and, for the first time, correctly demonstrates that the turbulent Prandtl number is not constant near a wall. Therefore, any heat transfer model that assumes a constant $Pr_t$ is not likely to be valid, even for simple pipe flows like the one considered here. Further evidence in support of this conclusion can be gleaned from a comparison of the present model calculations and the calculations using a constant $Pr_t$ but with a near-wall turbulence model for the Reynolds stresses. The $\Theta^+$ and $\overline{v\theta}$ results are shown in Figs. 1 and 6, respectively. Clearly, the constant $Pr_t$ results are in poor agreement with measurements. The velocity field, however, is not affected by this assumption and the results are identical to those obtained from the present model.

Finally, the importance of modeling $\varepsilon_{i\theta}$ in the near-wall region is illustrated in Figs. 9 and 10. In these figures, the budgets of the heat fluxes, $\overline{u\theta}$ and $\overline{v\theta}$, are plotted. As expected, $-D^\nu_{i\theta}$ is balanced by $\varepsilon_{i\theta}$ in the very near-wall region, $y^+ < 5$ (Figs. 9 and 10). If $\varepsilon_{i\theta}$ is assumed to be zero in view of the isotropic turbulence argument, then the heat flux equations are out of balance near a wall and the calculated $\overline{u\theta}$ and $\overline{v\theta}$ values are likely to be incorrect. The correct modeling of $\Phi^*_{i\theta}$ in the near-wall region is also of importance to $\overline{u\theta}$ and $\overline{v\theta}$ (Figs. 9 and 10). Close to the wall, $y^+ < 10$, $\Phi^*_{2\theta}$ and $\varepsilon_{2\theta}$ are providing the balance to $P_{2\theta,1}$ and $P_{2\theta,2}$ in the $\overline{v\theta}$ budget (Fig. 10). If $\Phi^*_{2\theta,w}$ is taken to be zero, the budget of $\overline{v\theta}$ near the wall will be out of balance. In other words, the calculated $\overline{v\theta}$ with $\Phi^*_{i\theta}$ given by $\Phi_{i\theta}$ alone will be incorrect. On the other hand, $\varepsilon_{i\theta}$ and $D^\nu_{i\theta}$ vanish quickly as the flow moves away from the

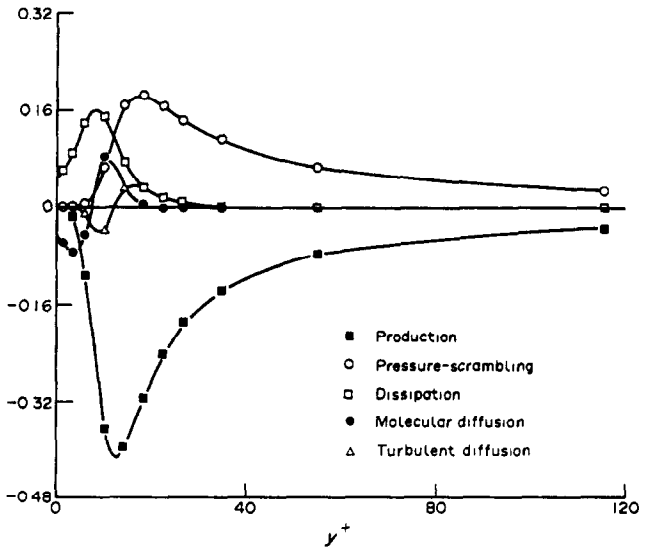


FIG. 9. Near-wall modeled behavior of the terms in the budgets of $\overline{u\theta}$.

wall. At $y^+ = 40$, the budgets in $\overline{u_i\theta}$ reduce to a balance between production and $\Phi^*_{i\theta}$. Convection of $\overline{u_i\theta}$ is of course zero for a fully-developed pipe flow. For this particular flow, turbulent diffusion of $\overline{u_i\theta}$ is essentially negligible beyond $y^+ = 20$, and is quite insignificant even for $y^+ < 20$. As a result, the model (12) proposed for $D^1_{i\theta}$ is more than satisfactory since it satisfies the near-wall behavior given in Table 1.

## CONCLUSIONS

The flow and heat transfer behavior near a wall is analysed by expanding the velocity components and temperature in terms of the coordinate normal to the wall. Consequently, the near-wall asymptotic behavior of all the terms except $\Phi^*_{i\theta}$ in the heat flux equations is known and the heat flux equations can be used to assess the near-wall asymptotic behavior of $\Phi^*_{i\theta}$. Based on this analysis, near-wall models are formulated for the molecular diffusion, dissipation and pressure-scrambling terms to give a new near-wall closure for the heat flux equations. All these models, except the molecular diffusion model, have the property of correctly approaching their respective high-Reynolds-number models far away from the wall; thus the conventional high-Reynolds-number closure of the heat flux transport equations can be recovered. The new near-wall heat flux closure is used in conjunction with a near-wall Reynolds-stress closure to calculate fully-developed pipe flows with uniform heat addition. Comparisons with experimental data show that the calculations are in excellent agree-

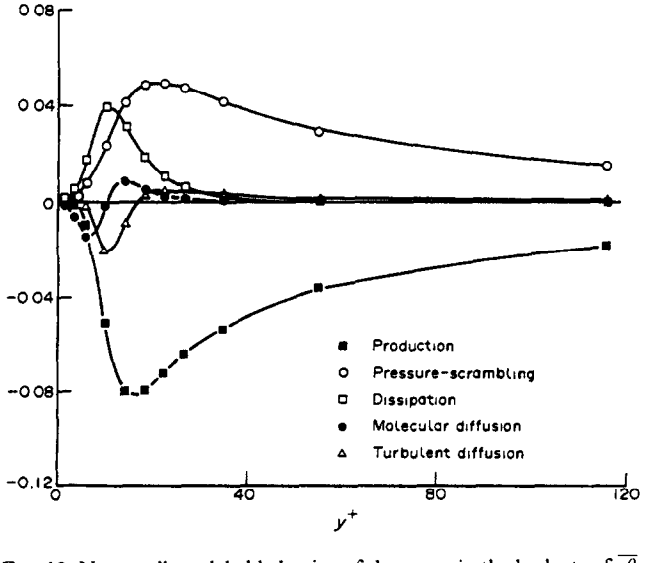


FIG. 10. Near-wall modeled behavior of the terms in the budgets of $\overline{v\theta}$.

ment with near-wall measurements, especially the normal heat flux. On the other hand, calculations based on a near-wall Reynolds-stress closure and a constant turbulent Prandtl number formulation for the normal heat flux are in poor agreement with measurements. This shows that the turbulent Prandtl number concept is not suitable for heat transfer calculations, even for fully-developed pipe flows.

The closure results show that the turbulent Prandtl number is not constant in the near-wall region. Instead, the turbulent Prandtl number increases steeply as the wall is approached. The present study also lends credence to the speculation that heat flux transport is more complicated than momentum transport and is more likely to be influenced by two or more time scales instead of one. Consequently, all conventional high-Reynolds-number models for the dissipation and pressure-scrambling terms in the heat flux equations are not very appropriate. Heat transfer modeling can be improved by formulating more appropriate dissipation and pressure-scrambling models. Once these models are available, the present methodology can again be applied to derive an asymptotically correct near-wall closure for the heat flux equations.

*Acknowledgements*—Research support from the Naval Weapons Center, China Lake, California under contract No. N60530-85-C-0191 and the David Taylor Naval Ship Research and Development Center, Annapolis, Maryland under contract No. N00167-86-K-0075 is gratefully acknowledged.

## REFERENCES

1. B. E. Launder, On the computation of convective heat transfer in complex turbulent flows, *J. Heat Transfer* **110,** 1112–1128 (1988).
2. Y. G. Lai and R. M. C. So, On near-wall turbulent flow modeling, *J. Fluid Mech.*, submitted for publication (1989).
3. R. M. C. So, Y. G. Lai, B. C. Hwang and G. J. Yoo, Low-Reynolds-number modelling of flows over a backward-facing step, *ZAMP* **39,** 13–27 (1988).
4. R. M. C. So and G. J. Yoo, Low-Reynolds-number modelling of turbulent flows with and without wall transpiration, *AIAA J.* **25,** 1556–1564 (1987).
5. B. E. Launder, Numerical computation of convective heat transfer in complex turbulent flows: time to abandon wall functions? *Int. J. Heat Mass Transfer* **27,** 1485–1491 (1984).
6. K. Bremhorst and K. J. Bullock, Spectral measurements of temperature and longitudinal velocity fluctuations in fully developed pipe flow, *Int. J. Heat Mass Transfer* **13,** 1313–1329 (1970).
7. K. Bremhorst and K. J. Bullock, Spectral measurement of turbulent heat and momentum transfer in fully developed pipe flow, *Int. J. Heat Mass Transfer* **16,** 2141–2154 (1973).
8. A. D. Carr, M. A. Connor and H. O. Buhr, Velocity, temperature and turbulence measurements in air for pipe flow with combined free and forced convection, *J. Heat Transfer* **95,** 445–452 (1973).
9. L. E. Hochreiter and A. Sesonske, Turbulent structure of isothermal and non-isothermal liquid metal pipe flow, *Int. J. Heat Mass Transfer* **17,** 113–128 (1974).
10. N. Shima, A Reynolds-stress model for near-wall and low-Reynolds-number regions, *J. Fluids Engng* **110,** 38–44 (1988).
11. W. Rodi, Recent developments in turbulence modelling, *Proc. 3rd Int. Symp. on Refined Flow Modelling and Turbulence Measurements*, Tokyo, 26–28 July (1988).
12. B. E. Launder and D. P. Tselepidakis, Contribution to the second-moment modelling of sublayer turbulent transport, *Proc. Zaric Memorial International Seminar on Wall Turbulence*, Dubrovnik, Yugoslavia. Hemisphere, Washington, DC (1988).
13. T. H. Shih and J. L. Lumley, Influence of time scale ratio on scalar flux relaxation: modelling Sirivat and Warhaft's homogeneous passive scalar fluctuations. *J. Fluid Mech.* **162,** 211–222 (1986).
14. B. E. Launder, Heat and mass transport. In *Turbulence—Topics in Applied Physics* (Edited by P. Bradshaw), Vol. 12, pp. 232–287. Springer, Berlin (1976).
15. Y. Nagano and C. Kim, A two-equation model for heat transport in wall turbulent shear flows, *J. Heat Transfer* **110,** 583–589 (1988).
16. M. Prud'homme and S. Elghobashi, Turbulent heat transfer near the reattachment of flow downstream of a sudden pipe expansion, *Numer. Heat Transfer* **10,** 349–368 (1986).
17. A. S. Monin, On the symmetry of turbulence in the surface layer of air, *IZV Atm. Oceanic Phys.* **1,** 45–54 (1965).
18. C. duP. Donaldson, Calculation of turbulent shear flows for atmospheric and vortex motions, *AIAA J.* **10,** 4–12 (1971).
19. O. Zeaman and J. L. Lumley, Buoyancy effects in entraining turbulent boundary layers. In *Turbulent Shear Flows—I*, pp. 295–306. Springer, Heidelberg (1979).
20. J. W. Baughn, M. A. Hoffman, B. E. Launder and D. S. A. Samaraweera, Three-dimensional turbulent heat transport in pipe flow: experiment and model validation, ASME Paper No. 78-WA-HT-15 (1978).
21. B. E. Launder and D. S. A. Samaraweera, Application of a second-moment turbulence closure to heat and mass transport in thin shear flows—I. Two-dimensional transport, *Int. J. Heat Mass Transfer* **22,** 1631–1643 (1979).
22. G. J. Yoo and R. M. C. So, Variable density effects on axisymmetric sudden-expansion flows, *Int. J. Heat Mass Transfer* **32,** 105–120 (1989).
23. R. E. Johnk and T. J. Hanratty, Temperature profiles for turbulent flow of air in a pipe—I. The fully developed heat transfer region, *Chem. Engng Sci.* **17,** 867–879 (1962).
24. M. Hishida, Y. Nagano and M. Tagawa, Transport processes of heat and momentum in the wall region of turbulent pipe flow, *Proc. 8th Int. Heat Transfer Conf.* (Edited by C. L. Tien *et al.*), Vol. 3, pp. 925–930. Hemisphere, Washington, DC (1986).
25. B. E. Launder, G. J. Reece and W. Rodi, Progress in the development of a Reynolds-stress turbulence closure, *J. Fluid Mech.* **68,** 537–566 (1975).
26. J. Kim, P. Moin and R. Moser, Turbulence statistics in fully developed channel flow at low Reynolds number, *J. Fluid Mech.* **177,** 133–186 (1987).
27. N. N. Mansour, J. Kim and P. Moin, Reynolds-stress and dissipation-rate budgets in a turbulent channel flow, *J. Fluid Mech.* **192,** 15–44 (1988).
28. R. G. Owen, An analytical turbulent transport model applied to non-isothermal fully-developed duct flows, Ph.D. Thesis, The Pennsylvania State University (1973).
29. B. E. Launder, Scalar property transport by turbulence, Rep. No. HTS/73/26, Dept. Mech. Engng, Imperial College, London (1973).
30. C. DuP. Donaldson, R. D. Sullivan and H. Rosenbaum, A theoretical study of the generation of atmospheric clear air turbulence, *AIAA J.* **10,** 162–170 (1972).
31. J. L. Lumley, Computational modelling of turbulent

flows. In *Advances in Applied Mechanics*. Vol. 18, pp. 123–126. Academic Press, New York (1978).
32. R. M. C. So and G. J. Yoo, On the modelling of low-Reynolds-number turbulence, NASA CR-3994 (1986).
33. J. Laufer, The structure of turbulence in fully developed pipe flow, NACA Rep. 1174 (1954).
34. S. E. Elghobashi and B. E. Launder, Turbulent time scales and the dissipation ratio of temperature variance in the thermal mixing layer, *Physics Fluids* **26**, 2415–2419 (1983).
35. J. L. Lumley, Turbulence modelling, *J. Appl. Mech.* **50**, 1097–1103 (1983).
36. F. H. Champagne, V. G. Harris and S. Corrsin, Experiments on nearly homogeneous turbulent shear flow, *J. Fluid Mech.* **41**, 81–139 (1970).
37. D. S. Johnson, Velocity and temperature fluctuation measurements in a turbulent boundary layer downstream of a stepwise discontinuity in wall temperature, *J. Appl. Mech.* **81**, 325–336 (1959).

## MODELISATION DES FLUX THERMIQUE TURBULENTS PRES DE LA PAROI

**Résumé**—Le comportement asymptotique près de la paroi des flux thermiques turbulents est analysé et le résultat est utilisé pour formuler une fermeture de second ordre pour le transfert thermique près de la paroi. L'analyse montre que les termes de la diffusion de pression et de la dissipation visqueuse sont de première importance dans la région pariétale et qu'ils doivent être correctement modélisés dans les équations de transport. On propose de nouveaux modèles qui satisfont le bilan pariétal exact entre diffusion visqueuse, dissipation visqueuse et diffusion de pression et ayant aussi des caractéristiques qui approchent les modèles à nombre de Reynolds élevé loin de la paroi. Des écoulements pleinement établis en canal avec flux thermique constant à la paroi sont choisis pour valider les modèles proposés. Les calculs montrent que les nouveaux modèles sont capables de bien représenter le comportement proche de la paroi. Néanmoins, ils dégagent l'état plutôt immature des modèles actuels des flux thermiques à grand nombre de Reynolds. La modélisation du terme de diffusion de pression montre qu'il a des effets sensibles sur le flux thermique calculé et on pense que ce terme est influencé par plus d'une échelle turbulente de temps. Enfin l'analyse vérifie aussi l'idée que le nombre de Prandtl turbulent n'est pas constant près de la paroi. Si le nombre de Prandtl turbulent est supposé constant les résultats obtenus ne s'accordent pas avec les mesures.

## MODELL ZUR BESCHREIBUNG DER WANDNAHEN VORGÄNGE BEI TURBULENTEM WÄRMETRANSPORT

**Zusammenfassung**—Das wandnahe asymptotische Verhalten bei turbulentem Wärmetransport wird analysiert. Das Ergebnis wird zur Formulierung einer Schließbedingung für die Turbulenz beim Wärmetransport nahe einer Wand benutzt. Dabei zeigt sich, daß die Terme für Druck und Dissipation im wandnahen Gebiet von besonders großer Bedeutung sind und in den Transportgleichungen sorgfältig einbezogen werden müssen. Es werden neue Modelle vorgeschlagen, die in Wandnähe das Gleichgewicht zwischen Impulstransport, Dissipation und Druck erfüllen und sich außerdem in großer Entfernung von der Wand an die entsprechenden herkömmlichen Modelle für große Reynolds-Zahlen anschließen. Vollständig entwickelte Rohrströmungen mit aufgeprägter Wärmestromdichte an der Wand werden zur Validierung des vorgeschlagenen Modells verwendet. Diese Berechnungen zeigen, daß die neuen Modelle das Verhalten nahe an der Wand sehr gut wiedergeben. Sie zeigen jedoch auch, daß Wärmetransportmodelle bei hoher Reynolds-Zahl ziemlich unausgereift sind. Schließlich bestätigt die Untersuchung, daß die turbulente Prandtl-Zahl nahe der Wand nicht konstant ist. Wenn die turbulente Prandtl-Zahl als konstant angenommen wird, weichen die Ergebnisse von entsprechenden Meßergebnissen ab.

## МОДЕЛИРОВАНИЕ ТУРБУЛЕНТНЫХ ТЕПЛОВЫХ ПОТОКОВ ВБЛИЗИ СТЕИКИ

**Аннотация**—Исследуется асимптотическое поведение турбулентных тепловых потоков вблизи стенки, и полученные результаты используются для формулировки тепловой модели второго порядка, предназначенной для моделирования переноса тепла вблизи стенки. Анализ показывает, что слагаемые, учитывающие диффузию давления и молекулярную диссипацию, являются наиболее важными в уравнениях для потока тепла в пристенной области и поэтому они должны быть адекватно смоделированы в указанных уравнениях. Предлагаются новые модели, удовлетворяющие условию баланса между молекулярной диффузией, "диссипацией" и диффузией давления вблизи стенки, и приближающиеся по адекватности к общепринятым моделям для больших значений турбулентных чисел Рейнольдса при больших расстояниях от стенки. Для проверки предложенных моделей рассмотрены полностью развитые течения в трубах с постоянным тепловым потоком на стенке. Расчеты показывают, что новые модели очень хорошо описывают тепловые потоки вблизи стенки. В то же время они указывают на недостаточную адекватность моделей для высоких значений турбулентного числа Рейнольдса. Показано, что моделирование слагаемого, учитывающего диффузию давления, оказывает существенное влияние на расчетное значение теплового потока и предполагается, что он зависит более чем от одного временного масштаба турбулентности. Анализ также подтверждает предположение о том, что значение турбулентного числа Прандтля вблизи стенки не является постоянным. Если $Pr$ принимается константой, то полученные результаты расчета расходятся с экспериментальными данными.